JACS
JOURNAL OF THE AMERICAN CHEMICAL SOCIETY
Article
pubs.acs.org/JACS

Carbon Monoxide Activation via O-Bound CO Using Decamethylscandocinium−Hydridoborate Ion Pairs

Andreas Berkefeld,[†] Warren E. Piers,*[,†] Masood Parvez,[†] Ludovic Castro,[§] Laurent Maron,*[,§] and Odile Eisenstein*[,¶]

[†]Department of Chemistry, University of Calgary, 2500 University Drive NW, Calgary, Alberta T2N 1N4, Canada
[§]LPCNO, Université de Toulouse, INSA, UPS, LPCNO, 135 avenue de Rangueil, F- 31077 Toulouse, France, and CNRS, LPCNO, F-31077 Toulouse, France
[¶]Institut Charles Gerhardt, Université Montpellier 2, CNRS 5253, cc 1501, Place E. Bataillon, F-34095 Montpellier, France

Supporting Information

ABSTRACT: Ion pairs $[Cp^*_2Sc]^+[HB(p\text{-}C_6F_4R)_3]^-$ (R = F, **1-F**; R = H, **1-H**) were prepared and shown to be unreactive toward D_2 and α-olefins, leading to the conclusion that no back-transfer of hydride from boron to scandium occurs. Nevertheless, reaction with CO is observed to yield two products, both ion pairs of the $[Cp^*_2Sc]^+$ cation with formylborate (**2-R**) and borataepoxide (**3-R**) counteranions. DFT calculations show that these products arise from the carbonyl adduct of the $[Cp^*_2Sc]^+$ in which the CO is bonded to scandium through the oxygen atom, not the carbon atom. The formylborate **2-R** is formed in a two-step process initiated by an abstraction of the hydride by the carbon end of an O-bound CO, which forms an η^2-formyl intermediate that adds, in a second step, the borane at the carbon. The borataepoxide **3-R** is suggested to result from an isomerization of **2-R**. This unprecedented reaction represents a new way to activate CO via a reaction channel emanating from the ephemeral isocarbonyl isomer of the CO adduct.

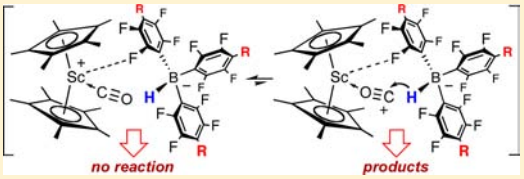

1. INTRODUCTION

Carbon monoxide is one of the most ubiquitous ligands in transition metal chemistry. Classical carbonyl complexes possess d electron configurations of $n \geq 2$ since π back-donation from filled metal d orbitals to the empty π antibonding (π^*) orbitals of the CO ligand is a major component of the M−CO bond (Figure 1a). Indeed, the metal−carbonyl bond is a textbook example[1] of the fundamental concept of synergic bonding involving ligand-to-metal σ donation and metal-to-ligand π back-donation in transition metal chemistry. Since the π^* accepting orbitals and the σ symmetric highest occupied molecular orbital (HOMO) of CO are more localized on the carbon atom, the vast majority of carbonyl compounds contain C-bound CO ligands. Even when the π^* component of the M−CO bond is diminished or eliminated, as in the so-called "non-classical" carbonyl complexes (Figure 1b), studied in much detail in the mid 1990s,[2] the carbonyl ligand binds to the metal through the orbitals associated with the carbon atom. In such compounds, the metal either possesses a d^0 electron configuration[3,4] (and therefore cannot engage in π bonding) or is a positively charged, highly electrophilic ion whose d electrons are too low in energy to interact strongly with the CO π^* orbitals.[5,6] Classical and nonclassical C-bonded CO complexes are distinguished by their C−O stretching frequencies in the infrared (IR) spectrum, with the former exhibiting values below and the latter above that of free CO (2143 cm^{-1}).

A third (and much more rare) mode of coordination for the CO ligand occurs when the lone pair on the oxygen atom engages in bonding to the metal, the O-bound isomer (Figure 1c).

Very few examples of authenticated monomeric O-bound complexes exist, and those that have been observed or postulated[7] occur only in highly electropositive metal fragments that are not capable of π-bonding, in other words, nonclassical systems. For example, Andersen et al.[8] have prepared mono and dicarbonyl adducts of decamethylytterbocene, Cp^*_2Yb (Cp^* is the pentamethylcyclopentadienide anion), whose IR spectroscopic stretching frequencies are *lower* than that of free CO, contrary to expectations for this metal fragment which cannot engage in π back-donation to the CO ligand(s). It has been shown computationally[9] that these observations are best explained by invoking O-bound structures, since O-bound ligands are expected to exhibit stretching frequencies below 2143 cm^{-1} despite the absence of π back-bonding. This system remains, to the best of our knowledge, the only *bona fide* example of an O-bound carbonyl complex that is stable under ambient conditions.

Metal complexes of carbon monoxide are significant not only for their role in the development of bonding models and theories but also because they are crucial intermediates in catalytic reactions that involve CO, an important C_1 synthon.

Received: January 18, 2012
Published: June 6, 2012

   dx.doi.org/10.1021/ja300591v | J. Am. Chem. Soc. 2012, 134, 10843−10851

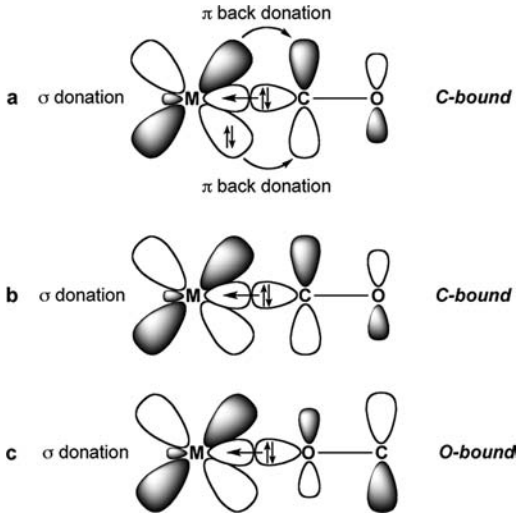

Figure 1. Bonding of carbon monoxide to a transition metal. (a) Classical bonding with σ donation from C to M and π backbonding from M to CO. (b) Nonclassical C-bound carbonyl in which the π backbonding component is absent or negligible. (c) O-bonded, or isocarbonyl, bonding in which the carbonyl oxygen atom is bonded to the metal.

Migratory insertion and deinsertion of CO into metal alkyl and metal hydrogen bonds is a primary reaction in organometallic chemistry and is the key step in widely deployed commercial processes such as olefin hydroformylation, the Monsanto acetic acid process, and Pauson–Khand chemistry, to name a few.[1] As such, its mechanism has been studied in detail;[10−13] it always involves C-bound carbon monoxide complexes of the type shown in Figure 1a,b, no exceptions. Thus, although the O-bound isomer appears to be energetically and kinetically accessible from the C-bound isomer in highly electropositive systems,[9] reactivity emanating from the O-bound isomer, which would be expected to be quite different from that of the C-bound form, has not been observed.[7]

New reactivity patterns require new ways to activate small molecules. In the mid 1990s, it was discovered that the strong Lewis acid *tris*-(pentafluorophenyl)borane, $B(C_6F_5)_3$, is capable of catalyzing the hydrosilylation of organic carbonyl functions[14] and imines[15] via activation of the Si–H bond of the silane,[16] rather than the Lewis basic organic function as might have initially been predicted. Subsequently, it was discovered that dihydrogen[17,18] can similarly be activated by $B(C_6F_5)_3$ in combination with an appropriately bulky Lewis base in systems described as "frustrated" Lewis pairs (FLPs),[19] since they are not able to form classical Lewis acid/Lewis base adducts. Such systems turn this frustration into useful bond activations of a fundamentally different nature than what was previously known. In the past few years, many groups have explored the scope of these reactions in terms of the molecules that can be activated by the FLPs;[20] however, CO appears to be reluctant to undergo binding or activation by the typical $B(C_6F_5)_3$/bulky Lewis base combinations explored so far.[21]

We have become interested in extending the FLP concept to include other strong Lewis acids, in particular cationic early transition metal complexes[22,23] partnered with a weakly coordinating but potentially functional anion. Here, the metal cation serves as the Lewis acid, and the counteranion is the bulky Lewis base partner that, upon activation of a substrate small molecule through coordination to the Lewis acidic transition metal ion, may transform it through transfer of a reactive anion to the substrate, for example a hydride or alkyl. Such systems may be thought of as "ionic FLPs", in contrast to the standard FLP systems that utilize neutral Lewis acids and bases to activate small molecules. Herein we report the development of an ionic FLP ensemble based on the decamethylscandocinium cation partnered with a weakly coordinating perfluoroarylhydrido borate anion and its use to activate carbon monoxide. The products formed strongly suggest that the CO is activated through its O-bound isomer, resulting in a new type of reactivity for coordinated CO. This proposal is corroborated by DFT computations.

2. RESULTS AND DISCUSSION

Decamethylscandocinium cations have been prepared by Hessen et al.[24] via protonolyis of the neutral $Cp^*_2ScCH_3$ compound (first reported by Bercaw et al. in 1987[25]) using ammonium salts of tetraarylborate counteranions, $[BAr_4]^-$ (Ar = C_6H_5 or C_6F_5). The products are contact ion pairs, in which the cationic scandium center is coordinated by meta and para C–H or C–F groups of one of the borate aryl rings. For Ar = C_6H_5, solvent-separated ion pairs are formed in the presence of fluoroarene solvents, which serve as donors to the highly Lewis acidic scandium center. These cations are thus highly electrophilic, but the counteranion partners in these instances are rather unreactive.

We were thus interested in the preparation of decamethylscandocinium ion pairs in which the counteranion consisted of potentially more reactive fluorarylhydridoborates. Although protonolyis routes akin to those used by Hessen et al. are feasible, the most convenient method for accomplishing this is shown in Scheme 1. Treatment of decamethylscandocene

Scheme 1

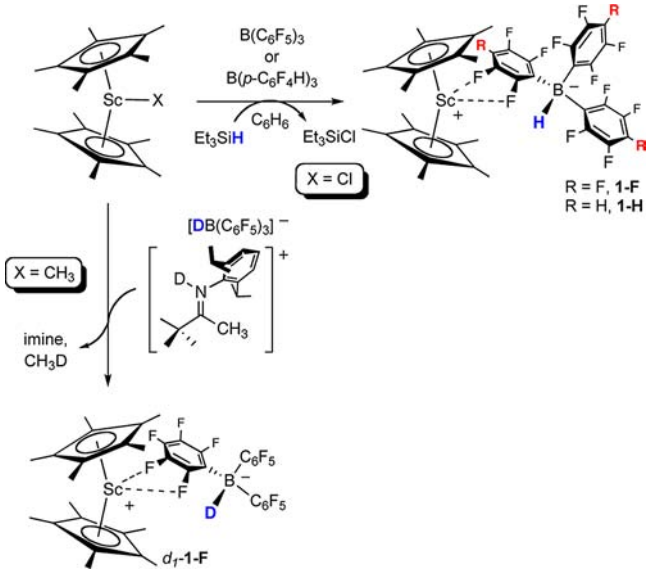

chloride, Cp^*_2ScCl, with one equivalent of $B(C_6F_5)_3$[26] or $B(p\text{-}C_6F_4H)_3$[27] and a slight excess of triethylsilane in benzene rapidly afforded the desired ion pairs as bright-yellow, microcrystalline precipitates in excellent isolated yields (>90%). Notably, no reaction is observed between Cp^*_2ScCl and silane in the absence of borane. The triethylchlorosilane byproduct was easily removed by washing the solid product with hexanes and drying it under vacuum. Alternatively, a

dx.doi.org/10.1021/ja300591v | J. Am. Chem. Soc. 2012, 134, 10843–10851

protonolysis route starting from the methyl derivative $Cp^*_2ScCH_3$ and employing the bulky iminium salt (2,6-di-*iso*-propylphenyl)-1,2,2-trimethylpropenylideneammonium deuterio-*tris*-(pentafluorophenyl)borate cleanly produces the ion pair d_1-**1-F**. This was the most convenient route to the deuterated ion pair, since the iminium reagent is readily available via FLP activation of D_2 using the free imine and $B(C_6F_5)_3$.[28] The imine liberated in the protonolysis reaction does not coordinate the scandium center and is removed by washing the product d_1-**1-F** with hexanes.

Ion pairs **1-R** (R = H or F, as defined in Scheme 1) were characterized by NMR spectroscopy and elemental analysis; furthermore, the structure of **1-F** was determined by X-ray crystallography (Figure 2). In the ^{11}B-decoupled ^{1}H NMR spectra, in addition to the intense singlet for the Cp* ligand protons, broad resonances at 4.13 (**1-F**) and 4.28 (**1-H**) were detected for the B–H protons; ^{11}B NMR spectra showed resonances typical of the $[HB(p\text{-}C_6F_4R)_3]^-$ anions at −25.3 and −24.6 ppm. The room temperature ^{19}F NMR spectra showed broadened resonances for the ortho- and meta-F nuclei, ($\nu_{1/2} \approx$ 145 Hz, **1-F**; $\nu_{1/2} \approx$ 490 Hz, **1-H**), and a sharp triplet resonance ($^3J_{F-F}$ = 21.1 Hz) for the para-F nuclei in the case of **1-F**. These observations are consistent with κ^2-*F* binding of the $[HB(p\text{-}C_6F_4R)_3]^-$ anions via the ortho and meta fluorine atoms, with the scandocinium cation moving from one ring to another on a time scale more rapid than that of the NMR spectroscopic experiment at room temperature. Due to low solubility in nonpolar solvents, this process could not be further defined via low-temperature NMR spectroscopy. In agreement with the solution NMR spectroscopic data, the solid-state structure of **1-F** shows that the contact between cation and anion occurs by coordination of an ortho and meta fluorine of one of the fluoraryl groups and not via the hydride, a situation likely dictated by steric factors. The Sc–F1 and Sc–F2 bond distances observed (2.3261(14) and 2.3396(16)Å, respectively) are completely consistent with those observed by Hessen et al.[24] in the related complexes $[Cp^*_2Sc(\kappa^2\text{-}F\text{-}1,2\text{-}F_2C_6H_4)]^+[B(C_6H_5)_4]^-$ and $[Cp^*_2Sc]^+[(\kappa^2\text{-}F\text{-}2,3\text{-}F_2C_6F_4)B(C_6F_5)_3]^-$ wherein the difluoroarene engages in a similar chelation of the cationic scandium center. The nonbonded Sc–H1 distance of 4.85(4)Å clearly shows that the hydride is not interacting with the scandium center.

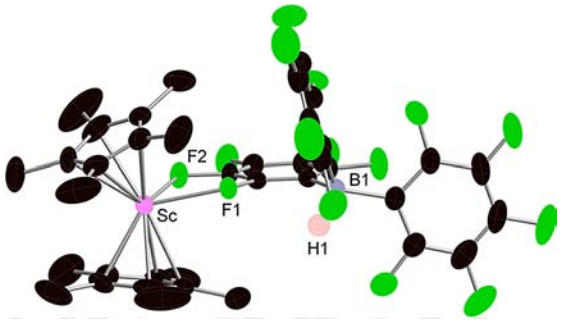

Figure 2. X-ray structure of **1-F** (thermal ellipsoids drawn to 50% probability level). All hydrogens except H1 omitted for clarity. Selected bond and nonbonded distances (Å): Sc–F1, 2.3261(14); Sc–F2, 2.3396(16); B1–H1, 1.14(3); Sc–H1, 4.853.

Despite the remote position of the hydride relative to the scandium, it is conceivable that the ion pairs **1-R** are in equilibrium with the neutral decamethylscandocene hydride, Cp^*_2ScH, and the free boranes $B(p\text{-}C_6F_4R)_3$. Hydride Cp^*_2ScH is a known species that is highly reactive toward deuterium gas, D_2, and α-olefins such as propene.[25,29] Thus, we treated bromobenzene solutions of **1-F** with 4 atm of D_2 (Scheme 2) and monitored the ^{1}H and ^{2}H NMR spectra for any indication of incorporation of deuterium into the hydridoborate anion. None was observed over the course of 48 h at room temperature; a similar experiment utilizing d_1-**1-F** and H_2 also gave no indication of isotope exchange between the deuterioborate and free dihydrogen. Furthermore, when the ion pairs were stirred in the presence of a large excess of propene, no change in the NMR spectra was seen over the course of 12 h. These experiments show that the hydridoborate counteranion does not reversibly transfer hydride to the scandium center and that the highly reactive Cp^*_2ScH species is not present in chemically meaningful quantities in solutions of the ion pairs.

Scheme 2

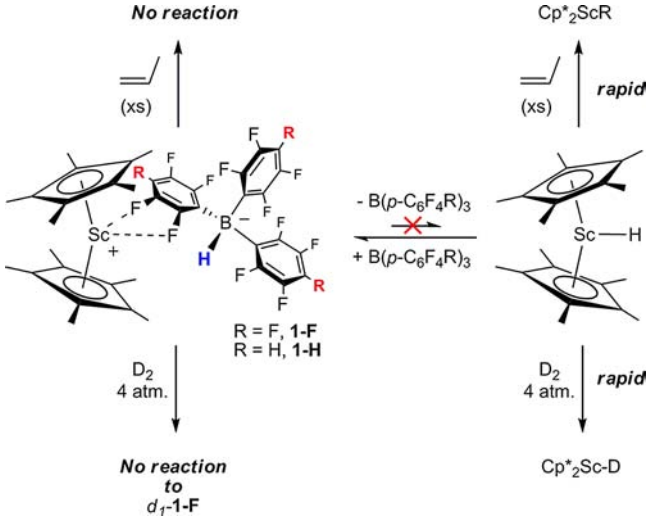

This was an important point to establish in light of the observed reactivity between ion pairs **1-R** with carbon monoxide. Separate experiments in which $Cp^*_2Sc\text{-}H$ is generated at low temperature via hydrogenolysis of $Cp^*_2Sc\text{-}CH_3$[25] and reacted with CO gave a complex product mixture, indicating that the putative formyl species is highly reactive. The propensity of $Cp^*_2Sc\text{-}H$ to form "tuck-in" complexes[25] and the "carbene-like" behavior of early metal formyl ligands[30,31] are likely factors in the intractable reaction chemistry of $Cp^*_2Sc\text{-}H$ with CO. It is thus significant that, even though this hydride is not accessible from ion pairs **1-R**, they react over the course of 12 h when exposed to 1 atm of CO gas to yield two distinct products, **2-R** and **3-R**, whose ratio is dependent on the nature of R as depicted in Scheme 3. By ^{1}H NMR spectroscopy (vide infra and Figure S1, Supporting Information [SI]), these reactions are essentially quantitative, with only ∼5% of a decomposition product of **1-R** in evidence along with **2-R** and **3-R** in the final product mixture.

In solution, the compounds are sufficiently stable to be fully characterized by ^{1}H, ^{11}B, ^{13}C, and ^{19}F NMR spectroscopy and IR spectroscopy; the molecular structure of compound **3-F** was identified concretely by single-crystal X-ray diffraction (Figure 3). The assignments were aided through the preparation of ^{13}C-labeled materials prepared by performing the reaction with isotopically enriched carbon monoxide, ^{13}CO (99%), and

dx.doi.org/10.1021/ja300591v | J. Am. Chem. Soc. 2012, 134, 10843–10851

Scheme 3

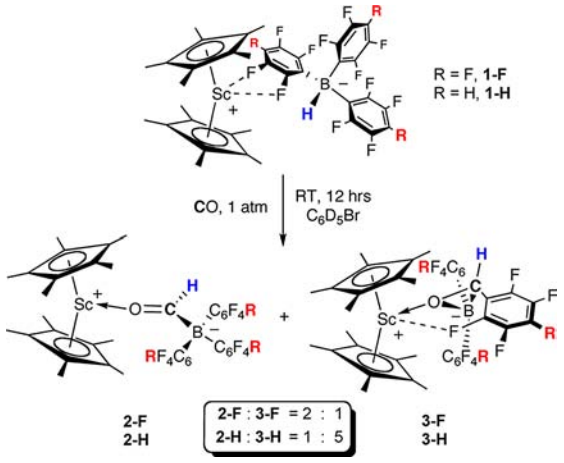

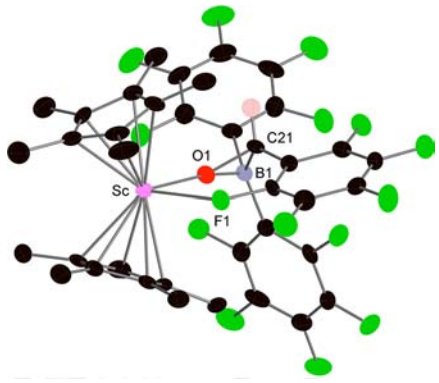

Figure 3. X-ray structure of **3-F** (thermal ellipsoids drawn to 50% probability level). All hydrogens except H bonded to C21 are omitted for clarity. Selected bond distances (Å) and angles (deg): Sc−F1, 2.320(4); Sc−O1, 2.187(4); B1−O1, 1.522(8); B1−C21, 1.559(9); O1−C21, 1.478(7). B1−C21−O1, 60.1(4); C21−O1−B1, 62.6(4); O1−B1−C21, 57.3(4).

through the use of d_1-**1-F**. The spectroscopic data is similar for both R = F and H, and only the data for compounds **2-F** and **3-F** will be discussed in detail. In the case of compound **2-F**, the assignment of its structure as the contact ion pair, in which the counteranion is the *tris*-(pentafluorophenyl)formylborate shown, is based primarily on the NMR and IR spectroscopic data obtained for the compound; the precise structural details of the contact between the cation and anion are not known experimentally. Although secondary Sc−F contacts are plausible, no evidence for this exists in the ^{19}F NMR spectrum of the compound, which shows a trio of sharp multiplet signals for the ortho, para, and meta fluorines of three equivalent C_6F_5 rings even at low temperature (203 K). Furthermore, the computed structure (vide infra) does not indicate such secondary stabilization. ^{1}H and ^{13}C NMR spectra, however, are diagnostic for a formylborate counteranion. A downfield signal at 11.80 ppm in the ^{1}H NMR spectrum that correlates to a resonance at 266.3 ppm in the ^{13}C NMR spectrum ($^1J_{CH}$ = 151 Hz) is consistent with the presence of a formyl group that is derived from the hydride of the borate counteranion in **1-F** and the added CO. This is corroborated by the absence of the resonance at 11.80 ppm when d_1-**1-F** is reacted with CO. Furthermore, one-bond coupling between the formyl carbon atom and boron-11 ($^1J_{CB}$ = 50.5 Hz) is observed, showing that this carbon is directly bonded to boron. Additionally, a two-bond coupling constant of 11.4 Hz is observed between the formyl hydrogen and the ^{11}B isotope of the borate boron. Correspondingly, the ^{1}H-coupled ^{11}B NMR spectrum showed a doublet coupling in the resonance at −13.3 ppm, in accord with boron in a four-coordinate, anionic borate environment, and distinctly different from the characteristic resonance for the hydridoborate anion at −25.3 ppm. Also consistent with the proposed structure is a band of moderate intensity at 1603 cm^{-1} in the IR spectrum of the product mixture, assignable to the C═O stretching frequency for the coordinated formyl group on the basis of a shift to 1567 cm^{-1} in the ^{13}C-labeled isotopomer.

The nature of product **3-F** is less straightforwardly assigned on the basis of its NMR spectroscopic data, although these data are fully consistent with the structure as determined by X-ray analysis on a small sample of single crystals obtained by selective crystallization of **3-F** from the product mixture. This unusual species may be described as a contact ion pair between $[Cp^*_2Sc]^+$ and a borataepoxide anion derived from CO and the hydridoborate anion of **1-F**. As can be seen in the thermal ellipsoid diagram of Figure 3, the core of the counteranion is a three-membered ring formed from B1, C21, and O1; ^{13}C-labeling shows that C21 is derived from CO, while ^{2}H-labeling (starting from d_1-**1-F**) shows that the proton on C21 comes from the hydridoborate hydrogen. This methine unit gives rise to resonances at 4.31 ppm in the ^{1}H NMR spectrum and 60.5 ppm in the ^{13}C NMR spectrum, with a large $^1J_{CH}$ coupling constant of 161 Hz, characteristic of C−H groups in a three-membered ring. The ^{11}B resonance at −8.6 ppm is very broad, but consistent with retention of a borate boron center, shifted downfield due to the oxygen donor. As might be expected, the ^{19}F NMR spectrum is complex, exhibiting significant broadening in the room-temperature spectra. However, upon cooling to 203 K a spectrum consistent with the molecule's structure is obtained, with two separate sets of resonances for the diastereotopic C_6F_5 groups directly bonded to boron, and three signals, integrating to 2:1:2 fluorines, for the C_6F_5 group attached to C21.

While these products are unusual, particularly the borataepoxides **3-R**, they have been mentioned as potential intermediates to explain products obtained in the carbonylation of alkali metal hydridoborate reagents such as $[Li]^+[HBEt_3]^-$. In an early study, Hubbard speculated[32] that a lithium borate with a borataepoxide structure must be present during the carbonylation of $[Li]^+[HBEt_3]^-$ to account for the observation of trimethylsilyl ethyl(1-ethylpropyl)borinate upon quenching of the reaction with Me_3SiCl. Here, the observation of a B−O bond in the product, rather than the expected C−O bond can be explained by the intermediacy of a borate with a B−O−C ring, (i.e., a borataepoxide), but the species was only characterized by ^{1}H-decoupled ^{11}B NMR spectroscopy via a signal at −2.7 ppm—strikingly similar to what we observe for compounds **3-R**. In other metal hydride-induced carbonylations of trialkylboranes,[33] formyl borates have been proposed to be intermediates but have not been observed. Kabalka was able to generate acyl borates through reactions of acyl lithium reagents with trialkylboranes at −115 °C,[34] but these rearrange rapidly upon warming. Thus, compounds **2-R** and **3-R** are unique in that they are stable in solution and provide confirmation of the earlier ideas of Hubbard. However, in light of these earlier precedents, it is significant that neither the $[TMPH]^+$ (TMP = 2,2,6,6-tetramethylpiperidine)[35] nor potassium salts of the perfluoroarylhydridoborate anion $[HB(C_6F_5)_3]^-$ react with

dx.doi.org/10.1021/ja300591v | J. Am. Chem. Soc. 2012, 134, 10843−10851

CO in bromobenzene, indicating that the decamethylscandocinium cation is essential for the observed reactivity.

The mechanism by which these unusual products are formed is of considerable interest. While the formyl borate ion pairs **2-R** could conceivably arise via "normal" CO insertion into the scandium hydride bond of Cp^*_2Sc-H (via a C-bound nonclassical CO complex) followed by abstraction of the formyl group by borane, this is not possible on the basis of the control experiments described above, since Cp^*_2Sc-H is not present. The products therefore arise via direct reaction of CO with ion pairs **1-R**, implying that CO interacts in some way with the electrophilic scandium center in the cation and is activated to accept the hydride from the borohydride anion. Since no intermediates were detected in the spectra of the ongoing reactions, this mechanistic hypothesis was explored using density functional theory (DFT) computations on the fully fluorinated compound **1-F** and CO.[36] The picture that emerges is that of these products arising from the O-bound isocarbonyl adduct of the decamethylscandocinium ion as depicted in Scheme 4; although the O-bound isomers **1-R·OC** are less stable than the C-bond isomers **1-R·CO**, no path that originated from the C-bound isomers was identified. The O-bound species, on the other hand, are close enough in energy to be accessible and directly lead to transition states that furnish the product **2-F**. Moreover, a low-energy path from **2-F** to **3-F** is also identifiable, and the computations imply that the two compounds are in equilibrium. The Gibbs energy profile for the reaction, with the energy of **1-F·CO** as energy reference, is depicted in Figure 4.

Scheme 4

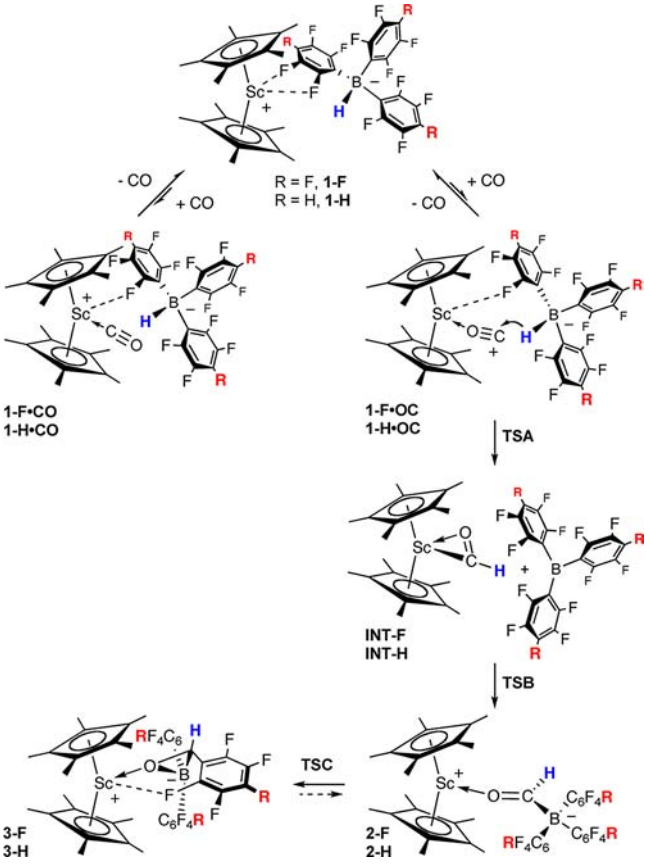

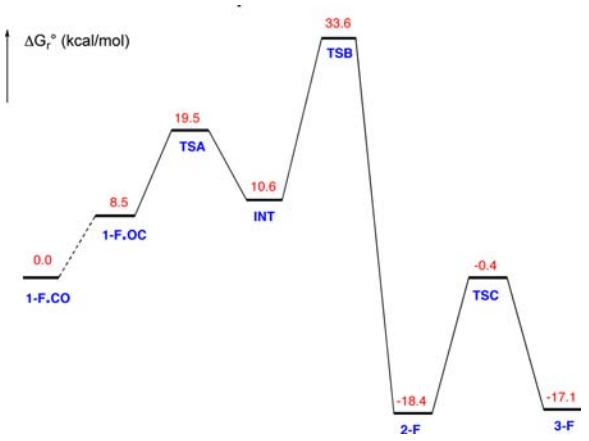

Figure 4. Gibbs energy profile for the transformation of **1-F·CO** in **2-F** and **3-F**. The isomerization of **1-F·CO** into **1-F·OC** occurs most likely by way of CO decoordination−coordination, and no transition state could be located.

The calculated structure of **1-F** is close to that obtained by X-ray crystallography; in particular the Sc−F1 and Sc−F2 distances of 2.29 and 2.41 Å are close to the experimental values of 2.3261(14) and 2.3396(16), respectively. Upon coordination of CO to form **1-F·CO**, the coordination mode of the $[HB(C_6F_5)_3]^-$ anion changes from κ^2- as in **1-F** to a κ^1-linkage in which only the ortho F1 is in the coordination sphere of Sc with a Sc−F1 distance of 2.259 Å and an angle Sc−F1−C(aryl) of 170°; the meta F2 is far from Sc (Figure S2 [SI]). In **1-F·CO**, the Sc−C distance is 2.336 Å, and the binding energy of C-bound CO is 6.7 kcal mol^{-1}. The Gibbs energy of the O-coordinated complex, **1-F·OC**, is 8.5 kcal mol^{-1} higher than that of the C-bound; the transition state connecting these two isomers[37] could not be identified, and thus it is presumed that they interconvert via CO dissociation/association.

A two-step reaction transforms **1-F·OC** into **2-F**. The O-coordinated CO ligand abstracts a hydride from $[HB(C_6F_5)_3]^-$ to form an η^2-formyl intermediate that is 10.6 kcal mol^{-1} above the energy reference. The transition state, **TSA**, of the hydride abstraction has a Gibbs energy of 19.5 kcal mol^{-1} and connects **1-F·OC** with the formyl intermediate. The next elementary step is the addition of the borane to the carbon of the formyl ligand. The corresponding transition state, **TSB**, is 33.6 kcal mol^{-1} above the energy reference and connects the formyl intermediate to observed product **2-F**.

The geometries of **TSA** and **INT** are given in Figure 5. **TSA** has a bent O-coordinated CO with an Sc−O bond length of 2.265 Å, an O−C bond length of 1.193 Å, and a C−O−Sc angle of 102.6°. The H of the borohydride is 1.431 Å from C, and the B−H−C angle is 167.9°. The hydride transfer occurs in the plane bisecting the $Cp^*_{centroid}$−Sc−$Cp^*_{centroid}$ equatorial plane. Interestingly, the hydride that does *not* transfer from the borohydride anion to Sc in **1-F** *does* transfer to the O−C ligand bound to Sc. In **TSA**, the position of the hydride relative to the OC ligand shows that the hydride maximizes its interaction with the π^*CO orbital that is in the equatorial plane (H···C−O angle of 109.3°) and minimizes its overlap with the carbon lone pair that points away from the OC ligand. The transfer of the hydride to CO occurs with a relatively low energy barrier because the electrophilicity of this ligand is enhanced by its coordination to the cationic, electron-deficient Sc center. In the η^2-formyl complex, **INT**, the Sc−O, Sc−C, and C−O bond distances are 2.214, 2.160, and 1.247 Å, respectively. The C−

dx.doi.org/10.1021/ja300591v | J. Am. Chem. Soc. 2012, 134, 10843−10851

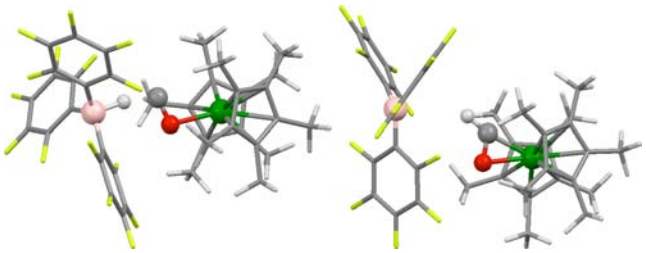

Figure 5. Geometries of **TSA** (left) and **INT** (right). Sc green, C gray, B pink, H white. See Figure 4 and Scheme 3 for labeling. Selected geometrical parameters (distances in Å, angles in degrees): **TSA**: B−H 1.366, H···C 1.431, C−O 1.193, O−Sc 2.265, C−O−Sc 102.6, H···C−O 109.3°. **INT**: B···H 3.241 Å, C−O 1.247, Sc−O, 2.214, Sc−*C* = 2.160, H−C−Sc 168.7, H−C−O 115.0.

O−Sc and O−C−Sc angles have the acute values of 71 and 75.8°, respectively. In contrast, the angles involving the hydrogen of the formyl group shows some geometrical features revealing of its reactivity behavior since the hydrogen is almost "*trans*" to Sc (Sc−C−H angle of 168.7°) but the H−C−O angle is 115°, indicative of an sp^2-hybridized carbon. These angles at the formyl carbon indicate that the carbon lone pair does not point toward Sc but away from the three-membered metallacycle ring. This is consistent with a nucleophilic property of the formyl carbon. Similar structural features were obtained in a computational study of the reaction of Cp_2CeH with CO. The intermediate, resulting form the insertion of CO in the CeH bond, $Cp_2Ce(\eta^2\text{-HCO})$, cleaves H_2 in a heterolytic manner.[38] Related geometrical features have been obtained for the $Cp'_2Ce(\eta^2\text{-}H_2COMe)$ complex where the two hydrogens, the C, and Ce are almost coplanar. This species, which is an intermediate of reaction of the cerium hydride with MeOMe, reacts at the carbon of the $\eta^2\text{-}H_2COMe$ ligand with the nonfluorinated Lewis acid BPh_3.[39]

The geometries of **TSB** and **2-F** are given in Figure 6. In **TSB**, the Sc−C bond is mostly broken, but the B−C bond is

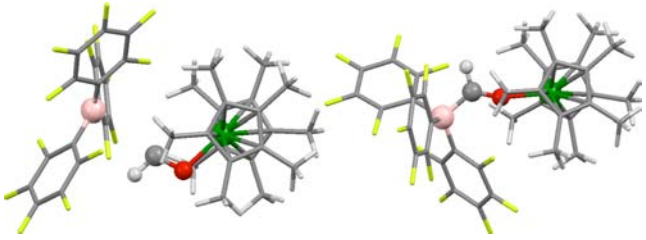

Figure 6. Geometries of **TSB** (left) and **2-F** (right). Sc: green, C gray, B pink, H white. See Figure 4 and Scheme 3 for labeling. Selected geometrical parameters (distances in Å, angles in degrees): **TSB**: Sc−O 2.11, Sc−C 2.70, B···C 3.1, Sc−O−C 109.0, H−CO 109.4. **2-F**: Sc−O 2.09, O−C 1.246 Å, B−C 1.641; Sc−O−C 162.5, H−C−O 114.7, H−C−B 118.0.

still forming, as suggested by the distances of 2.70 Å and 3.1 Å, respectively. The Sc−O−C and H−C−O angles of ∼109.2° are also indicative of the lack of Sc−C interaction and of a C lone pair that points more toward B than Sc. The geometry of **2-F** shows a formylborate with no unexpected structural features, in full agreement with that proposed on the basis of the spectroscopic data (*vide supra*). The Sc−O−C angle of 162.5° and the Sc−O distance of 2.09 Å suggests substantial π-donation from the carbonyl function to the cationic metal center, as has been observed in other ketone adducts of metallocenium cations.[40] This perhaps accounts for the lack of secondary F→Sc interactions in this structure.

Calculations show that **3-F**, which is 1.3 kcal mol^{-1} above **2-F**, is formed by isomerization of **2-F** with a transition state, **TSC**, whose Gibbs energy is −0.4 kcal mol^{-1} below the energy reference and 22 kcal mol^{-1} above that of **2-F**. The geometries for the transition state between **2-F** into **3-F**, **TSC**, and **3-F** are shown in Figure 7. At **TSC**, one of the C_6F_5 group bridges the

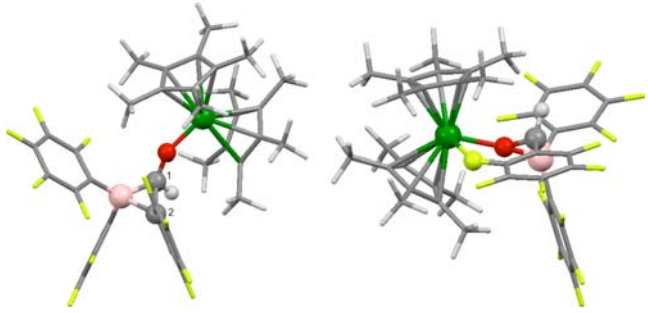

Figure 7. Geometries of **TSC** (left) and **3-F** (right). Sc green, C gray, B pink, H white. See Figure 4 and Scheme 3 for labeling. Selected geometrical parameters (distances in Å, angles in degrees): **TSC**: Sc−O 2.021, O−C1 1.329, B−C1 1.539, B−C2, 1.902, C1−C2 1.738, B···O 2.584, B−C1−O 128°. **3-F**: Sc−F 2.429, Sc−O 2.175, B−O 1.535, B−C 1.580, O−C 1.450.

C1−B bond, and the B−C1−O angle is 128° which is associated with a B···O distance of 2.584 Å. Thus, in **TSC**, there is not yet any interaction between B and O, and the B−O bond is formed during the descent from the transition state. The computed structure of **3-F** agrees well with that determined by X-ray crystallography, with the only significant discrepancy being observed for the computed Sc−F1 distance that is 2.429 Å vs the experimental value of 2.320(4) Å; bonds that are weak are often calculated to be too long.

While the computations suggest that **2-F** and **3-F** are in equilibrium, with a barrier of 17−18 kcal mol^{-1} between them, we have no conclusive experimental evidence for exchange between the two compounds. Exchange NMR spectroscopy experiments showed that the rate of exchange was outside of the time scale window for this technique. The ratio of the two compounds did not change significantly with varying temperature, indicating that $\Delta S°$ for this equilibrium is close to zero. When crystals of **3-F** isolated from the product mixture were redissolved in C_6D_5Br, small amounts of **2-F** were present and grew in slowly over time; however, the final ratio observed in the forward ratio was not established, so this result too is inconclusive.

Collectively, the computations show that, while the O-bonded CO is not the preferred coordination between **1-F** and CO, the isocarbonyl complex **1-F·OC** (which is a shallow secondary minimum) still determines the reactivity of **1-R** with CO. Carbon monoxide has a lone pair of σ-symmetry on C and O and two orthogonal π orbitals. In the usual C-bound coordination of CO to a metal complex, the higher lying C-localized σ lone pair is used for binding to the metal, and the π^*_{CO}, which are more on C than O (see Figure 1), are used for back-donation from the metal when the metal d orbitals are occupied. The highest occupied and lowest unoccupied orbitals of CO are thus used for the metal−CO interaction. However, in the O-bonded CO complex, the C-localized lone pair is directed away from the metal, and the coordination of the

dx.doi.org/10.1021/ja300591v | *J. Am. Chem. Soc.* 2012, 134, 10843−10851

oxygen to the metal increases the electron-withdrawing character of the oxygen. This results in a lowering of the energy of all orbitals, and in particular of the empty π^*_{CO}, which are localized on the carbon. The isocarbonyl complex thus has a doubly occupied σ-type lone pair localized on carbon and two empty π^*_{CO}-type orbitals with a strong carbon contribution. This makes the O-bound CO ligand a strong enough electrophile to engage in an interaction with a nucleophile. The geometry of **TSA** highlights the Lewis acid character of the O-bound CO since the hydride is positioned to maximize the interaction with the π^*_{CO} orbital. While the hydride does not transfer from the borohydride to the Sc center probably because the distance Sc···H in **1-F** is too long, the presence of the CO ligand decreases the distance between the Lewis base and the Lewis acid, making the hydride transfer a possible reaction. This transfer is not very demanding in energy, but all intermediates, **1-F·OC** and **INT**, have a Gibbs energy above that of **1-F·CO** and also that of separated **1-F** and CO. Thus, none of the intermediates can accumulate sufficiently to be detectable by spectroscopic means.

The formation of **2-F** is significantly exoergic so that the overall reaction is favorable. The overall activation barrier of 33.6 kcal mol^{-1} above **1-F·CO** is compatible with the experimental conditions (12 h at rt). Calculations show that **3-F** is obtained from isomerization of **2-F**. The difference in energy between the two isomers is small, and the accuracy of the calculated difference in energy between **2-F** and **3-F** is not sufficient to comment on the experimental ratio of **2-F** and **3-F** and also on that of **2-H** and **3-H**. In all cases these energy values are compatible with ratio of **2-R** and **3-R** that is small.

3. CONCLUSIONS

In conclusion, we have observed the activation and (albeit stoichiometric) functionalization of carbon monoxide using a strategy that employs an ion pair as an "ionic frustrated Lewis pair" in which the Lewis acidic site remains accessible for the incoming CO ligand and in which the weakly coordinating anion is capable of contributing chemically to the activation process. A key aspect of this chemistry is that the highly electropositive—and oxophilic—nature of the decamethylscandocinium cation employed allows for access of the ephemeral O-bound isomer of a carbonyl complex and that it is from this complex that the observed chemistry emanates. This is, to our knowledge, a new mode of reactivity for transition metal coordinated carbon monoxide and the first to arise from an O-bound isocarbonyl complex. The ionic nature of compounds **1-R** opens this unusual reaction channel by keeping the reacting B−H and B−C bonds in close proximity to the carbon of the O-bound carbonyl ligand, which due to its energetic nature must have a relatively short lifetime. In this sense, the reaction is a homogeneous analog of other systems in which chemistry occurs in a physically confined environment, for example the pores of a zeolite, or the active site of an enzyme. Here, the electrostatic pocket of the ion pair defines the confined but reactive volume and orients the CO ligand through O-bounding that allows for this unprecedented reaction to be observed. The potential for this concept in catalytic processes is currently being explored for the activation and conversion of carbon monoxide and other small molecules.

4. EXPERIMENTAL SECTION

4.1. Preparation of Ion Pairs 1-R. *4.1.1. Silane Route.* In a glovebox, a benzene (2.5 g) solution of $B(C_6F_5)_3$ (512 mg, 1.00 mmol) and Et_3SiH (140 mg, 1.20 mmol) was added to a solution of Cp^*_2ScCl (344 mg, 0.98 mmol) in benzene (2.5 g; 20 mL screw cap vial) by pipet at room temperature (rt). The color of the reaction mixture changed instantaneously from dark to bright yellow. The resulting solution is carefully layered with hexanes (∼10 mL), and the vial sealed and kept at rt overnight. Bright yellow prismatic crystals separated and were recovered by careful removal of the pale-yellow mother liquor by pipet, washed with hexanes (2 mL, 3 times), and dried under dynamic vacuum. Yield: 760 mg, 0.88 mmol, 89% **1-F***0.5C_6H_6. $^1H\{^{11}B\}$ NMR (400 MHz, C_6D_5Br, 298 K): δ 7.20 (s, 3H, 0.5 equiv. C_6H_6), 4.13 (br s, $\nu_{1/2} \approx 20$ Hz, 1H, B-*H*), 1.58 (s, 30H, $C_5(CH_3)_5$); ^{19}F NMR (376 MHz, C_6D_5Br, 298K): δ −133.9 (br s, $\nu_{1/2} \approx 145$ Hz, 6F, *o*-F), −160.3 (t, J = 21.1 Hz, 3F, *p*-F), −166.8 (br s, $\nu_{1/2}$ ∼145 Hz, 6F, *m*-F); ^{11}B NMR (128 MHz, C_6D_5Br, 298K): δ −25.3 (br d, line width ≈ J); $^{13}C\{^1H\}$ NMR (101 MHz, C_6D_5Br, 298 K): δ 128.3 (C_6H_6), 126.5 ($C_5(CH_3)_5$), 10.2 ($C_5(CH_3)_5$) [^{13}C resonances of C_6F_5 rings were not detected]; IR (KBr): 2387 cm^{-1} (ν_{B-H}); analysis (calcd, found for $C_{41}H_{34}BF_{15}Sc$): C (56.77, 56.45), H (3.95, 4.02). Yield for **1-H** (0.14 mmol Sc): 110 mg (0.14 mmol), quant., thin yellow needles. $^1H\{^{11}B\}$ NMR (400 MHz, C_6D_5Br, 298 K): δ 6.66 (tt, J = 10.1, 7.5 Hz, 3H, *p*-C_6F_4H), 4.28 (br s, $\nu_{1/2}$ ∼20 Hz, 1H, B-*H*), 1.59 (s, 30H, $C_5(CH_3)_5$); ^{19}F NMR (376 MHz, C_6D_5Br, 298K): δ −134.2 ($\nu_{1/2}$ ∼490 Hz, 6F, *o*-F), −144.4 ($\nu_{1/2}$ ∼490 Hz, 6F, *m*-F); ^{11}B NMR (128 MHz, C_6D_5Br, 298K): δ −24.6 (br s, $\nu_{1/2}$ ∼120 Hz); $^1H,^{13}C$-HSQC, HMBC spectroscopy (400 MHz, C_6D_5Br, 298K): δ 148.5 and 146.2 (C_{aryl}-F), 125.9 ($C_5(CH_3)_5$), 100.9 (C_{aryl}−H), 10.1 ($C_5(CH_3)_5$) [^{13}C NMR resonance of B-bound *ipso*-C was not detected]; IR (KBr): 2410 cm^{-1} (ν_{B-H}); analysis (calcd., found for $C_{38}H_{34}BF_{12}Sc$): C (58.93, 58.84), H (4.43, 4.45).

4.1.2. Protonolysis Route (d_1-1-F). A 100 mL round-bottom flask equipped with a magnetic stir bar was charged with $Cp^*_2ScCH_3$ (111 mg, 0.34 mmol) and (2,6-di-*iso*-propylphenyl)-1,2,2-trimethylpropenylideneammonium deuterio-*tris*-(pentafluorophenyl)borate (260 mg, 0.34 mmol), and was attached to a swivel-frit assembly. The apparatus was removed from the glovebox, evacuated on the vacuum line, and the solids cooled to −78 °C (acetone/dry ice) for 20 min, and toluene (20 mL) was finally condensed onto the solids. The cold bath was removed 10 min after solvent transfer and the reaction mixture allowed to slowly warm to rt, yielding an dark yellow solution. Toluene was removed after 30 min at rt under dynamic vacuum and pentane was condensed onto the semisolid residue at −78 °C. After warming to rt in a water bath, the mixture was vigorously triturated until a yellow powder separated (∼60 min). The latter solid was isolated by filtration, washed with pentane (3 times) cycled within the swivel-frit to completely remove the 1,1,1-trimethyl-2-(2,6-diisopropylphenyl)-iminopropane byproduct, and finally dried under dynamic vacuum for 3 h. In the glovebox, the solid product was recrystallized from benzene/hexanes at −35 °C, yielding bright-yellow prismatic crystals. The mother liquor was removed by pipet, and the crystals were washed with hexanes (2 mL, 3 times) and dried under dynamic vacuum (30 min). Yield: 200 mg (0.23 mmol), 68% d_1-**1-F***0.5C_6H_6. ^1H NMR data were found to match those of **1-F**, except for the B−H resonance. Analysis (calcd, found for $C_{41}H_{33}DBF_{15}Sc$): C (56.70, 55.40), H (4.06, 4.11).

4.2. Reactions of 1-R with CO. In a glovebox, a 100 mL pressure-resistant glass vessel equipped with a micro stir bar was charged with **1-F***0.5C_6H_6 (23 mg, 26 μmol) and C_6D_5Br (0.85 g, 0.54 mL), yielding a bright-yellow solution. The vessel was sealed, removed from the glovebox, and connected to the high vacuum line. The solution was frozen in a −78 °C (acetone/dry ice) cold bath and the headspace evacuated. The vacuum manifold of the line was charged with a ∼1:1 mixture of ^{13}C-labeled and unlabeled CO, and the gases were allowed to mix for 3 h. The obtained gas mixture was admitted to the evacuated vessel cooled to −196 °C. The vessel was sealed and slowly warmed to rt and the reaction mixture stirred overnight. After careful removal of CO gas from the headspace, the vessel was taken into the glovebox and the solution transferred into a sealable NMR tube. The ^1H NMR spectrum (Figure S1 [SI]) revealed the formation of a 2:1 mixture of **2-F**/**3-F** with a $^{13}C/^{12}C$ ratio of 1:1.5. A mixture of **2-F**/**3-F** can be isolated as a pale-yellow solid (>70% by mass balance) by

removal of bromobenzene under dynamic vacuum and trituration of the residual oil with pentane (1 mL) at −78 °C (acetone/dry ice), filtration, and drying under dynamic vacuum. Single crystals of **3-F** suitable for X-ray diffraction were grown from layering a benzene solution of the solid with hexanes, but quantities of these crystals sufficient for elemental analysis were not obtainable. ^{13}C-**2-F**: $^{1}H\{^{19}F\}$ NMR (400 MHz, C_6D_5Br, 298 K): δ 11.80 (dq, J_{H-C} = 151 Hz, J_{H-B} = 12 Hz, 1H, $[O{=}C(H)B(C_6F_5)_3]^-$), 1.43 (s, 30H, $C_5(CH_3)_5$); ^{19}F NMR (282 MHz, C_7D_8, 203 K): δ −130.4 (m, 6F, *o*-F), −156.9 (m, 3F, *p*-F), −162.9 (m, 6F, *m*-F); ^{11}B NMR (128 MHz, C_6D_5Br, 298 K): δ −13.5 (br dd, J_{B-C} = 51 Hz, J_{B-H} = 12 Hz); ^{13}C NMR (101 MHz, C_6D_5Br, 298 K): δ 266.3 (dq, J_{C-H} = 151 Hz, J_{C-B} = 51 Hz), 124.0 (s, $C_5(CH_3)_5$), 10.3 ($C_5(CH_3)_5$) [^{13}C NMR resonances of C_6F_5 rings were not detected]; IR (KBr): 1603 cm^{-1} ($\nu_{O=12C(H)B}$), 1567 cm^{-1} ($\nu_{O=13C(H)B}$). d_1-**2-F**: ^{2}H NMR (61 MHz, C_6H_5Br, 298 K): δ 11.77 (br, $\nu_{1/2} \approx 17$ Hz). ^{13}C-**3-F**: $^{1}H\{^{19}F\}$ NMR (400 MHz, C_6D_5Br, 298 K): δ 4.31 (d, J = 160.8 Hz, 1H, *cyclo*-O-C*H*(C_6F_5)−$B(C_6F_5)_2$), 1.67 and 1.55 (s each, 15H each, $C_5(CH_3)_5$); ^{19}F NMR (282 MHz, C_7D_8, 203 K): C-bound C_6F_5: δ −126.4 (m, 2F, *o*-F), −152.0 (m, 1F, *p*-F), −161.9 (m, 2F, *m*-F), B-bound C_6F_5: (a) δ −132.5 (m, 1F, *o*-F), −136.5 (m, 1F, *o*′-F), −156.2 (m, 1F, *p*-F), −161.2 (m, 1F, *m*-F), −163.3 (m, 1F, *m*′-F), (b) δ −136.8 (m, 1F, *o*-F), −155.2 (m, 1F, *p*-F), −159.4 (m, 1F, *m*-F), −163.2 (m, 1F, *m*′-F), −169.6 (m, 1F, *o*′-F); ^{11}B NMR (128 MHz, C_6D_5Br, 298 K): δ −8.6 (br, $\nu_{1/2} \approx 280$ Hz); ^{13}C, $^{13}C\{^{1}H\}$ NMR (101 MHz, C_6D_5Br, 298 K): δ 144.5 and 137.7 (*o*-, *m*-C *cyclo*-O-CH(C_6F_5)−$B(C_6F_5)_2$), 124.2 and 123.8 (s each, $C_5(CH_3)_5$), 118.6 (*ipso*-C *cyclo*-O-CH(C_6F_5)−$B(C_6F_5)_2$), 60.5 (d, J = 161 Hz, *cyclo*-O-CH(C_6F_5)−$B(C_6F_5)_2$), 11.2 and 11.1 (s each, $C_5(CH_3)_5$) [^{13}C NMR resonances of *p*-C (*cyclo*-O-CH(C_6F_5)−$B(C_6F_5)_2$) and of B-bound C_6F_5 rings were not detected]. d_1-**3-F**: ^{2}H NMR (61 MHz, C_6H_5Br, 298 K): δ 4.26 (br, $\nu_{1/2} \approx 40$ Hz).

5. COMPUTATIONAL DETAILS

The Stuttgart−Dresden−Bonn Relativistic Large Effective Core Potential (RECP) was used to represent the inner shells of Sc with its associated basis set.[41] Fluorine atoms were treated with an effective core potential in conjunction with its associated basis set augmented by a set of d polarization functions.[42] The atoms B, C, O, and H were represented by an all-electron 6-31G(d, p) basis set.[43] Calculations were carried out at the DFT(B3PW91) level with *Gaussian09*.[44] The nature of the extrema (minimum or transition state) was established with analytical frequencies calculations, and the intrinsic reaction coordinate (IRC) was followed to confirm that the transition states connect to reactants and products. The zero-point energy (ZPE) and entropic contribution have been estimated within the harmonic potential approximation. The Gibbs free energies, G, were calculated at T = 298.15 K and p = 1 atm. The NBO analysis was carried out with the NBO program attached to *Gaussian09*.[45] Additional test calculations on the CO insertion in the BC bond were carried out with the DFT-D[46] and the MO6 functionals[47,48] to evaluate the consequence of a better representation of the weak interactions on the activation barriers. Similar results were obtained with all functionals.

■ ASSOCIATED CONTENT

Supporting Information

Crystallographic data files for **1-F** and **3-F**, additional experimental and spectroscopic details and tables of coordinates, energies E and Gibbs energies G in a.u. for all calculated structures and the full list of authors for ref 44. This material is available free of charge via the Internet at http://pubs.acs.org.

■ AUTHOR INFORMATION

Corresponding Author

wpiers@ucalgary.ca; Odile.Eisenstein@univ-montp2.fr

Notes

The authors declare no competing financial interest.

■ ACKNOWLEDGMENTS

Funding for the experimental work described was provided by the Natural Sciences and Engineering Research Council of Canada in the form of a Discovery Grant to WEP A.B. thanks the Deutsche Forschungsgemeinschaft for financial support in the form of a Postdoctoral Fellowship. L.C. thanks the Ministère de l'Enseignement Supérieur et de la Recherche for a Ph.D. fellowship. L.M. and O.E. thank the CNRS and the Ministère de l'Enseignement Supérieur et de la Recherche for funding. L.M. is a junior member of the Institut Universitaire de France. The CALMIP (Toulouse) and CINES (French National centre) are gratefully acknowledged for a generous donation of computational time.

■ REFERENCES

(1) Hartwig, J. F. *Organotransition Metal Chemistry: From Bonding to Catalysis*; University Science Books: Mill Valley, CA, 2010.
(2) Lupinetti, A. J.; Strauss, S. H.; Frenking, G. *Progress in Inorganic Chemistry*; John Wiley & Sons, Inc.: New York, 2001; p 1.
(3) Antonelli, D. M.; Tjaden, E. B.; Stryker, J. M. *Organometallics* **1994**, *13*, 763.
(4) Guo, Z.; Swenson, D. C.; Guram, A. S.; Jordan, R. F. *Organometallics* **1994**, *13*, 766.
(5) Hurlburt, P. K.; Anderson, O. P.; Strauss, S. H. *J. Am. Chem. Soc.* **1991**, *113*, 6277.
(6) Willner, H.; Schaebs, J.; Hwang, G.; Mistry, F.; Jones, R.; Trotter, J.; Aubke, F. *J. Am. Chem. Soc.* **1992**, *114*, 8972.
(7) Frey, A. S.; Cloke, F. G. N.; Hitchcock, P. B.; Day, I. J.; Green, J. C.; Aitken, G. *J. Am. Chem. Soc.* **2008**, *130*, 13816.
(8) Selg, P.; Brintzinger, H. H.; Schultz, M.; Andersen, R. A. *Organometallics* **2002**, *21*, 3100.
(9) Maron, L.; Perrin, L.; Eisenstein, O.; Andersen, R. A. *J. Am. Chem. Soc.* **2002**, *124*, 5614.
(10) Butler, I. S.; Basolo, F.; Pearson, R. G. *Inorg. Chem.* **1967**, *6*, 2074.
(11) Noack, K.; Calderazzo, F. *J. Organomet. Chem.* **1967**, *10*, 101.
(12) Bock, P. L.; Boschetto, D. J.; Rasmussen, J. R.; Demers, J. P.; Whitesides, G. M. *J. Am. Chem. Soc.* **1974**, *96*, 2814.
(13) Wax, M. J.; Bergman, R. G. *J. Am. Chem. Soc.* **1981**, *103*, 7028.
(14) Parks, D. J.; Piers, W. E. *J. Am. Chem. Soc.* **1996**, *118*, 9440.
(15) Blackwell, J. M.; Sonmor, E. R.; Scoccitti, T.; Piers, W. E. *Org. Lett.* **2000**, *2*, 3921.
(16) Parks, D. J.; Blackwell, J. M.; Piers, W. E. *J. Org. Chem.* **2000**, *65*, 3090.
(17) Welch, G. C.; Juan, R. R. S.; Masuda, J. D.; Stephan, D. W. *Science* **2006**, *314*, 1124.
(18) Welch, G. C.; Stephan, D. W. *J. Am. Chem. Soc.* **2007**, *129*, 1880.
(19) Stephan, D. W. *Org. Biomol. Chem.* **2008**, *6*, 1535.
(20) Stephan, D. W.; Erker, G. *Angew. Chem., Int. Ed.* **2010**, *49*, 46.
(21) Dureen, M. A.; Stephan, D. W. *J. Am. Chem. Soc.* **2010**, *132*, 13559.
(22) Chapman, A. M.; Haddow, M. F.; Wass, D. F. *J. Am. Chem. Soc.* **2011**, *133*, 8826.
(23) Chapman, A. M.; Haddow, M. F.; Wass, D. F. *J. Am. Chem. Soc.* **2011**, *133*, 18463.
(24) Bouwkamp, M. W.; Budzelaar, P. H. M.; Gercama, J.; Del Hierro Morales, I.; de Wolf, J.; Meetsma, A.; Troyanov, S. I.; Teuben, J. H.; Hessen, B. *J. Am. Chem. Soc.* **2005**, *127*, 14310.
(25) Thompson, M. E.; Baxter, S. M.; Bulls, A. R.; Burger, B. J.; Nolan, M. C.; Santarsiero, B. D.; Schaefer, W. P.; Bercaw, J. E. *J. Am. Chem. Soc.* **1987**, *109*, 203.
(26) Piers, W. E. *Adv. Organomet. Chem.* **2005**, *52*, 1.
(27) Welch, G. C.; Prieto, R.; Dureen, M. A.; Lough, A. J.; Labeodan, O. A.; Holtrichter-Rossmann, T.; Stephan, D. W. *Dalton Trans.* **2009**, 1559.
(28) Chase, P. A.; Jurca, T.; Stephan, D. W. *Chem. Commun.* **2008**, 1701.

(29) Piers, W. E.; Shapiro, P. J.; Bunel, E. E.; Bercaw, J. E. *Synlett* **1990**, 74.
(30) Manriquez, J. M.; McAlister, D. R.; Sanner, R. D.; Bercaw, J. E. *J. Am. Chem. Soc.* **1978**, *100*, 2716.
(31) Fagan, P. J.; Moloy, K. G.; Marks, T. J. *J. Am. Chem. Soc.* **1981**, *103*, 6959.
(32) Hubbard, J. L. *Heteroat. Chem.* **1992**, *3*, 223.
(33) Hubbard, J. L.; Smith, K. *J. Organomet. Chem.* **1984**, *276*, c41.
(34) Kabalka, G. W.; Gotsick, J. T.; Pace, R. D.; Li, N.-S. *Organometallics* **1994**, *13*, 5163.
(35) Sumerin, V.; Schulz, F.; Nieger, M.; Leskelä, M.; Repo, T.; Rieger, B. *Angew. Chem., Int. Ed.* **2008**, *47*, 6001.
(36) The results are discussed using Gibbs energies in kcal mol^{-1}, calculated at 298 K and one atmosphere of pressure (see Supporting Information for further details).
(37) Wesolowski, S. S.; Galbraith, J. M.; Schaefer, H. F. *J. Chem. Phys.* **1998**, *108*, 9398.
(38) Werkema, E. L.; Maron, L.; Eisenstein, O.; Andersen, R. A. *J. Am. Chem. Soc.* **2007**, *129*, 2529.
(39) Werkema, E. L.; Andersen, R. A.; Yahia, A.; Maron, L.; Eisenstein, O. *Organometallics* **2009**, *28*, 3173.
(40) Sun, Y. M.; Piers, W. E.; Yap, G. P. A. *Organometallics* **1997**, *16*, 2509.
(41) Dolg, M.; Wedig, U.; Stoll, H.; Preuss, H. *J. Chem. Phys.* **1987**, *86*, 866.
(42) Maron, L.; Teichteil, C. *Chem. Phys.* **1998**, *237*, 105.
(43) Hariharan, P. C.; Pople, J. A. *Theor. Chem. Acc.* **1973**, *28*, 213.
(44) Frisch, M. J.; et al. *Gaussian 09*, Revision A.2; Gaussian Inc.: Wallingford CT, 2009. See SI for complete citation.
(45) *NBO*, version 3.1; Glendening E. D.; Reed A. E.; Carpenter, J. E.; Weinhold, F.
(46) Grimme, S.; Antony, J.; Ehrlich, S.; Krieg, H. *J. Chem. Phys.* **2010**, *132*, 154104.
(47) Zhao, Y.; Truhlar, D. G. *J. Chem. Phys.* **2006**, *125*, 194101.
(48) Zhao, Y.; Truhlar, D. G. *Acc. Chem. Res.* **2008**, *41*, 157.